5.1   AN AUTOMATED, OPERATIONAL TWO HOUR CONVECTIVE WEATHER FORECAST
FOR THE CORRIDOR INTEGRATED WEATHER

Robert A. Boldi*, M. M. Wolfson, W.J. Dupree, R. J. Johnson Jr., K.E. Theriault, B.E. Forman,
and C.A. Wiilson,
MIT Lincoln Laboratory, Lexington, Massachusetts

1.   INTRODUCTION†

The FAA Aviation Weather Research Program (AWRP) is an initiative of the Weather and Flight Service Systems Integrated Product Team, AUA-400. One of the goals of the AWRP is to create accurate and accessible forecasts of hazardous weather tailored to the needs of the aviation community. Pursuant to this goal, the AWRP has sponsored the collaboration of the Research Applications Program (RAP) of the National Center for Atmospheric Research (NCAR), the Aviation and Forecast Research Divisions at the NOAA Forecast Systems Laboratory (FSL), the Weather Sensing Group of the Massachusetts Institute of Technology's Lincoln Laboratory (MIT/LL) and the National Severe Storm Laboratory (NSSL) on a Product Development Team (PDT).

This Convective Weather PDT is developing an automated system that combines real-time weather-radar data with the current "state-of-the-art" convective weather prediction algorithms to produce forecasts of convective weather for the heavily traveled air traffic routes in the Great Lakes/Northeast corridor (Chicago to New York). This Regional Convective Weather Forecast (RCWF) will be provided to traffic flow management decision-makers as part of the proof-of-concept Corridor Integrated Weather System (CIWS), which began operations in July 2001 with a 1-hr animated Regional Convective Weather Forecast (RCWF).

Specifically, in 2002, RCWF will forecast the probability of NWS-level 3 and greater radar-reflectivity for 8 successive 15-minute periods up to 2 hours into the future. Predictions will update every 5 min. These forecasts are presented in a variety of formats, each tailored to a specific class of user. The users of these forecasts span the spectrum of aviation-concerned government and private sector positions (i.e. FAA Command Center, TMUs, FSS, ARTCC-CWSUs, and airline pilots and dispatchers).

*Corresponding author address: Robert A. Boldi, MIT Lincoln Laboratory, 244 Wood Street, Lexington, MA 02420-9108, email: bobb@ll.mit.edu

Relative to currently available forecasts, the accuracy of these forecasts are being improved via higher quality and resolution input data as well as advances in the scientific understanding of both the causative atmospheric processes and their predictability. The accessibility of these forecasts is being improved via dissemination of user-specific information that permits time-critical decisions to be made in light of these forecasts with a minimum of meteorological interpretation.

This forecast system utilizes the method of combining interest maps at each forecast epoch. The interest maps are based on feature extraction using functional template correlation and advection. Each feature contributes differently at each forecast epoch. Accordingly, this system emphasizes small scale forcing (e.g. storm initiation, growth, and dissipation) during the 0 - 60 min forecast range and larger scale forcing (e.g. fronts) for the 60 - 120 min forecast range, and each forcing is advected with it own motion field.

This paper now reviews (1) the basic meteorological data utilized in the forecast, (2) the features having the greatest influence at each forecast horizon, and (3) the methods used to combine the features in order to generate the sequence of forecasts. Finally, we will discuss the Lincoln Laboratory vision of the role that weather information can play in reducing air traffic congestion in the en-route air space.

2.   METEOROLOGICAL DATA UTILIZED

NEXRAD base data (reflectivity and radial velocity) are acquired via dedicated communication lines from the 21 NEXRADs located throughout the Great Lakes/Northeast corridor region as shown in Figure 1.
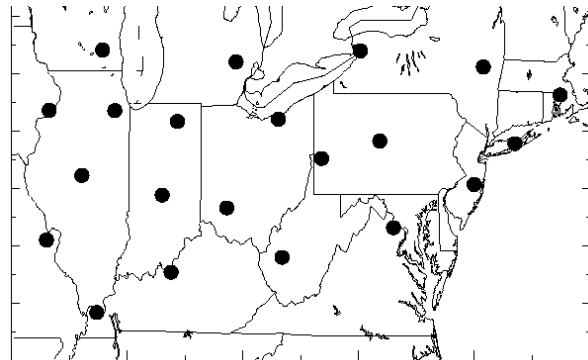

Figure 1. Location of NEXRAD systems.

In addition to NEXRAD data, GOES-8 data are acquired via a dedicated ground station wherein the visible and IR data are ground-registered, mapped to a standard CIWS grid, and advected to the standard analysis-time periods (every five minutes). Thermodynamic data are derived from the 20 km resolution, "Rapid Update Cycle" Model (RUC). These data are acquired via FTP from FSL as it becomes available. Selected fields from this data set are remapped to the standard CIWS grid and advected to the standard analysis time periods. The RUC model provides a variety of outputs (e.g. the analysis fields, the 1-hr, 3-hr and 6-hr forecast fields), each of which is independently processed. The amount of agreement between these fields at the analysis time is used as a measure of the reliability or weight given to interest maps derived from these data.

3. SKILL AT VARIOUS FORECAST EPOCHS

The following table presents our *a-priori*, subjective analysis of the relative skill levels of the various components of a 2-hr convective weather forecast. As noted from the bottom line of this table (the Relative Score), the skill of a forecast falls off rapidly with time.

Feature	Forecast Epoch (minutes)				
	15	30	60	90	120
Improve Cell Motions	3	2	1	0	0
Improve Line Storm Motions	3	3	2	2	2
Radar-Based Growth Trends	3	1	0	0	0
Radar-Based Decay Trends	3	3	2	1	0
Gust Front Forcing	2	2	1	0	0
Synoptic Scale Forcing	2	2	2	2	2
Diurnal Anticipation	1	1	1	1	1
Relative Score	**17**	**14**	**9**	**6**	**5**

Table 1. Relative skill of various components of a two-hour convective weather forecast.

The consequences of this for longer time horizon forecasts will be discussed in the final section of this paper. For now, we note that this table serves as a high level introduction to the components of our forecast system. Each component is a set of interest maps (one for each forecast epoch); the individual components are now described.

4. METHODS USED TO CREATE 2-HR RCWF

The 2-hr RCWF builds on the foundations established by the baseline 1-hr TCWF ("baseline TCWF"), and the "Enhanced-TCWF" (TCWF) the salient features of which have been described elsewhere and are (1) the growth and decay storm tracker (Wolfson *et al*, 1999) for

the "baseline TCWF" and (2) the storm classifier and multi-scale tracker (Dupree *et al*, 2002) for the "enhanced-TCWF" (TCWF).

The storm classifier/multi-scale tracker first classifies regions into one of the following "weather-types": Line-Storm, Small-Cell, Large-Cell, or Stratiform. It then advects components of the image with weather-type specific motion measured for each weather-type whenever required.

Base Map Construction

The most important data utilized by this system are maps of VIL spanning the CIWS domain, created at 5-minute intervals (the standard analysis times) by advecting and mosaicking the VIL maps from each of the 21 NEXRADs in CIWS. The data are advected to the analysis time using the weather-type specific motion vectors obtained from the multi-scale tracker. These time-aligned data are then mosaicked using the *maximum-plausible* rule which states that where more than one NEXRAD has a good viewing angle, choose the highest value of VIL if at least one other NEXRAD provides confirming evidence in the form of a slightly lower value of VIL. If no NEXRAD can confirm the highest value, then this maximum value is rejected as probable clutter or artifact, and the process is repeated.

Interest Feature Construction

(1) Persistence. Given knowledge of the current VIL map and its motion, the 2-hr RCWF begins by using weather-type specific persistence weighting functions to initialize each pixel of the forecast maps for each of the forecast periods. Symbolically, this can be stated as equation 1a.

$$I(\delta t) = F_0(V, WxT, \delta t) + \ldots \quad (1a.)$$

Where I is the probability of a given pixel having NWS-Level 3 or greater precipitation at forecast horizon δt; V is the current value of VIL at the pixel in question, WxT is the weather type at the pixel, and F_0 is a function that models the anticipated behavior of each class of weather-type over time. This function captures the long known result that intense, large (organized) precipitation patterns are the most likely to persist (Wilson, 1966); i.e. it returns a relatively large value (predicting persistence) for intense Line-Storms for all δt's and returns an increasingly negative value (predicting increasing decay) for Small-Cells as δt increases. The +… represents terms described next. In order to extend the forecast horizon out to 2 hours, we have added to the above persistence new maps of interest based on short-term growth and decay trends (trending), improved characterization of boundary layer and synoptic scale forcing, and diurnal anticipation.

(2) Trending. Persistence of trend is measured by differencing a NEXRAD-specific sequence of filtered, advected VIL images to produce a map of the changes in VIL (δV). The filter is an azimuthally-symmetric

Gaussian having a standard deviation of 13km that is convolved with the data. The previous analysis time's filtered image is advected forward to the current analysis time with weather-type specific motion vectors averaged over a time period that increases with the time horizon for which we make a forecast. These changes in VIL are then multiplied by a function that captures the potential for precipitation based on growth rate, weather-type, and forecast horizon and is represented by F_1 in eq. 1b.

$$I(t + \delta t = \quad F_0(V, WxT, \delta t)$$
$$+ \ \delta V * F_1(\delta V, WxT, \delta t) + \ldots \ (1b.)$$

Where F1 returns relatively large values for growing line storms and decaying Small Cells, and relatively small values for growing Small Cells.

(3) Forcing. After persistence and trending, we examine three products for organized patterns of growth that we interpret as evidence of frontal boundary layer forcing; i.e. we look for (a) linear patterns in the VIL growth field δV, (b) evidence of convergent boundaries in the NEXRAD radial velocities, and (c) organized lines of cumulus clouds.

3a) Linear growth in VIL. The δV map is examined for regions showing organized growth (positive interest), i.e. linearly-organized, isolated regions of growth on the scale of 30km x 60km and (b) regions showing unorganized growth (negative interest), i.e. small scale, isolated growth. These are represented by F2 and F3 respectively in eq. 1c.

$$I(t + \delta t) \ = \quad F_0(V, WxT, \delta t)$$
$$+ \quad \delta V \ * F_1(\delta V, WxT, \delta t)$$
$$+ \ F_2(I_{IsolatedLargeLineGrowth}, \delta t)$$
$$+ \ F_3(I_{IsolatedSmallCellGrowth}, \delta t)(1c).$$

3b) Fronts detected by NEXRAD-MIGFA. In addition to the VIL field, the radial velocity field of each NEXRAD is examined for evidence of organized boundary forcing (a.k.a. gust fronts). This has required significant improvements to the MIGFA algorithm as described by Troxel & Delanoy (1994). These changes have resulted in detecting greater lengths of gust front features - mainly by 1) use of an "adaptive" reflectivity thin-line detector which detects thin line signatures over a wide range of reflectivities, 2) extending the length of existing gust front detections via auxiliary interest maps, and 3) contextual "joining" of collinear, similarly-moving detected gust front segments.
The detected fronts are tracked over time and the past, present, and future positions of these fronts for each of the forecast time horizons are mapped onto the standard CIWS grid. The functional template applied to these maps has a maximum in the growth interest in those regions that are predicted to contain a gust front within a time window -10 to +5 minutes relative to the forecast horizon of the grid.

3c) Satellite Data. Further interest in organized growth is provided by reference to the satellite data. At each analysis period, the locations of cumulus clouds are detected using a texture-based functional template that is designed to detect regions of linearly aligned cumulus in the vicinity of gust fronts. The synoptic situation being tested for is shown in Figure 2, where the left side shows the plan view of an advancing gust front moving out ahead of a cluster of storms. In the right-hand image, the gust front is shown causing uplift, developing cumulus, and subsequently the first radar echo.
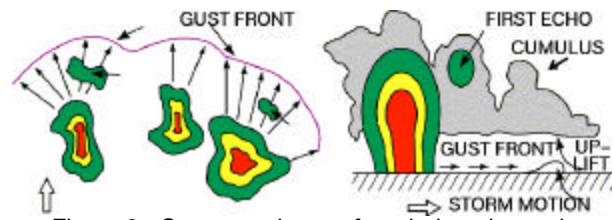

Figure 2. Storm-scale gust front induced growth.

(4) Diurnal Anticipation. Given the pronounced dependence that convection has on the time of day (with the minimum at 15:00Z and maximum at 21:00Z) a domain wide, time dependent function reflecting the averaged thunderstorm activity as a function of the time of day is added to the interest map.
The final conversion of a particular value of interest to the probability of NWS Level-3 is done by classifying the interest values into No, Low, and High probability based on an analysis of historical cases.

5. PERFORMANCE OF 2-HR RCWF

The addition of trending information to the RCWF system has improved our ability to anticipate decay of storms. One example of this is seen in Figure 3, where the left side (A) shows the 2-hr RCWF's predictions of the precipitation, and the right (B) is the forecast with the addition of trending interest (i.e. negative interest due to decay).
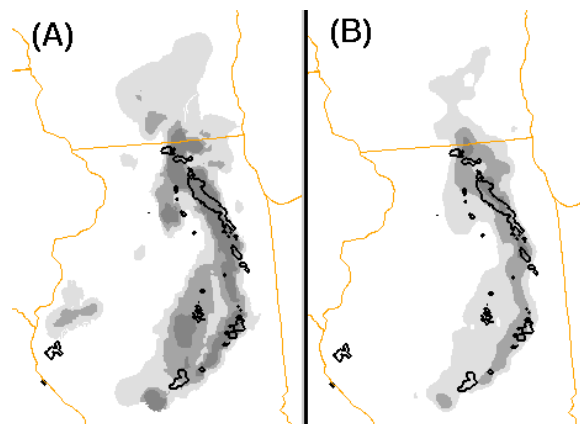

Figure 3. 2-hr forecasts on 7/18/01. (A) RCWF, (B) RCWF plus trending. (Black contours are the NWS level-3 verification regions).

6. THE FORECAST PRODUCTS

The 2-hr RCWF provides the users with two basic products. The first is a movie loop at 15-minute increments of the past hour of weather and the forecast maps for the next two hours. The forecast maps depict regions of low, moderate, and high probability of NWS Level-3 (or greater) convective weather, and explicitly portray the anticipated coverage patterns. The second product is the performances of the 30 and 60 minute forecast horizons; measured by comparing the current weather with past forecasts. Other products are being developed based on user feedback to these basic products.

7. LONGER-TIME FORECAST HORIZONS

Given the rapid fall off of skill with forecast horizon noted in Table 1, longer time horizon forecasts of convective precipitation (3 - 6 hrs) may not have the precision to be usefully presented on a map such as Figure 3. Instead, a ``regional penetrability'': a measure of likely route capacity in a weather-impacted region is required. The current Collaborative Convective Forecast Product (CCFP) gives some indication of this with the forecast storm height, trend, and coverage information as shown in Figure 4.
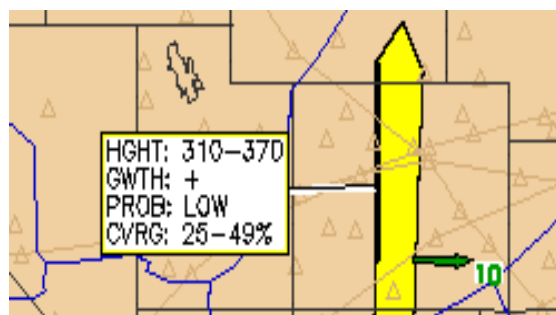

Figure 4. CCFP information box.

Algorithms need to be developed that can provide maps of traversable air traffic routes considering the weather at the origin at time of departure, the en-route weather during flight and the weather at the destination at the time of arrival.

To forecast such a route combines the problem of predicting convective weather patterns with the problems of relating this weather to (1) pilot behavior (Rhoda et al. 2002), (2) the geographical arrangement of ARTCCs and their sectors' capacities, and (3) the development of a ``risk mitigation plan'', i.e. a list of re-route options available in case a previous forecast proves faulty.

8. SUMMARY

Automated graphical forecasts of convective weather out to two hours are now possible and will be demonstrated in Summer 2002 as part of the CIWS operations. As the time horizon extends out much beyond this however, new display products will have to be invented to couple the understanding of the state of the atmosphere with the requirements of air-traffic management. We recognize a definite relationship between the forecast time horizon and the qualitative nature of the decisions made at that epoch.

9. REFERENCES

Dupree, W.J, R. Johnson Jr., M. M. Wolfson, K. E. Theriault, B. E. Forman, R.A. Boldi, and C. A. Wilson, 2002. Forecasting Convective Weather using Multi-scale Detectors and Weather Classification – Enhancements to the MIT Lincoln Laboratory Terminal Convective Weather Forecast. 10th Conference on Aviation, Range, and Aerospace Meteorology, these proceedings.

Rhoda, D., E. Kocab and M. Pawlak, 2002 "Aircraft Encounters With Thunderstorms in Enroute vs. Terminal Airspace Above Memphis, Tennesee", 10 Conference on Aviation, Range, and Aerospace Meteorology, American Meteorological Society, Portland, OR, 13-16 May 2002.

Troxel, S.W., and R.L. Delanoy, 1994: "Machine intelligent approach to automated gust front detection for Doppler weather radars," SPIE Proceedings: Sensing, Imaging, and Vision for Control and Guidance of Aerospace Vehicles, Volume 2220, pp. 182-193.

Wilson, James W., 1966. Movement and Predictability of Radar Echoes, U.S. Dept. of Commerce, Environmental Science Services Administration, Institutes for Environmental Research Technical Memorandum, IERTM-NSSL-28, Norman, OK.

Wolfson, M.M., B.E. Forman, R.G. Hallowell, and M.P. Moore, 1999: The Growth and Decay Storm Tracker. 8th Conference on Aviation, Range, and Aerospace Meteorology, Dallas, TX, pp 58-62.